www.ecjse.com
ISSN:2148-3736
El-Cezerî Fen ve Mühendislik Dergisi
Cilt: 3, No: 3, 2016 (417-427)

El-Cezerî Journal of Science and Engineering
Vol: 3, No: 3, 2016 (417-427)

ECJSE

Research Paper / Makale

Adsorption of Cr(VI) Ions on Magnetite Nano-Particles (Fe_3O_4): Kinetic and Thermodynamic Studies

Hakan ÇİFTÇİ*, Bahri ERSOY

Afyon Kocatepe University, Engineering Faculty, Mining Engineering Department, 03200 Afyonkarahisar/TURKEY
*hciftci@aku.edu.tr

Received/Geliş: 22.06.2016 **Revised/Düzeltme:** 23.08.2016 **Accepted/Kabul:** 31.08.2016

Abstract: This article intends to investigate the kinetic and thermodynamic properties of adsorption process of hexavalent chromium [Cr(VI)] ions on magnetite nano-particles (Fe_3O_4, MNPs). In accordance with this purpose, MNPs were synthesized by chemical co-precipitation method and characterized by FTIR, TEM and VSM methods at first. After that, a series of adsorption experiments were performed for removal of Cr(VI) ions from aqueous media by MNPs. Finally, thermodynamic and kinetic properties of Cr(VI) adsorption on MNPs were investigated. Mean particle size and magnetization saturation (Ms) of synthesized MNPs were about 15 nm and be 75 $emug^{-1}$, respectively. Under optimum adsorption conditions, adsorption capacity and Cr(VI) removal percentage were found to be 33.45 mg/g and 88%, respectively. According to calculated thermodynamic parameters after adsorption experiments, Cr(VI) adsorption process was a result of endothermic reactions. Langmuir and Freundlich isotherm models were investigated and it was observed that the removal of Cr(VI) could be better described by the Langmuir model. Kinetic investigations showed that the pseudo-second-order model have a better description of the Cr(VI) adsorption.

Keywords: Nano magnetite; Cr (VI); Adsorption isotherm; Adsorption kinetics; Adsorption thermodynamic.

Cr(VI) İyonlarının Manyetit Nano-Partikülleri (Fe_3O_4) Üzerine Adsorpsiyonu: Kinetik ve Termodinamik Çalışmalar

Özet: Bu çalışmada, hekzavalent krom [Cr(VI)] iyonlarının manyetit nano-partikülleri (Fe_3O_4, MNP) ile adsorpsiyonu prosesinin kinetik ve termodinamik özelliklerinin araştırılması amaçlanmıştır. Bu amaç doğrultusunda, ilk olarak kimyasal ikili çöktürme tekniği kullanılarak MNP sentezlendi ve elde edilen ürünler FTIR, TEM ve VSM gibi metotlar ile karakterize edildi. Daha sonra, sulu ortamdan Cr(VI) iyonlarının giderilmesi için MNP ile bir dizi adsorpsiyon deneyleri yapıldı. Son olarak da Cr(VI) iyonlarının MNP ile adsorpsiyonu prosesinin kinetik ve termodinamik çalışmaları yapıldı. Sentezlenen nano-partiküllerin ortalama tene boyutunun 15 nm ve mıknatıslanma doygunluğunun da 75 $emug^{-1}$ olduğu tespit edildi. Optimum adsorpsiyon şartlarında, adsorpsiyon kapasitesi ve Cr(VI) giderim yüzdesi sırasıyla 33.45 mg/g ve %88 olarak hesaplandı. Adsorpsiyon deneyleri sonrası hesaplanan termodinamik parametrelere göre MNP ile Cr(VI) adsorpsiyonu endotermik reaksiyonların sonucu oluşan bir proses olduğu söylenebilir. Langmuir ve Freundlich izoterm modelleri araştırıldı ve adsorpsiyon prosesinin Langmuir modeli ile daha iyi açıklanabilir olduğu tespit edildi. Kinetik araştırmalar sonucunda ise MNP ile Cr(VI) iyonlarının adsorpsiyonu için sözde-ikinci-derece kinetik model ile daha iyi bir açıklama getirilebilir.

Anahtar kelimeler: Nano manyetit; Cr(VI); Adsorpsiyon kinetiği; Adsorpsiyon termodinamiği.

How to cite this article
Çiftçi, H., Ersoy, B. "*Adsorption of Cr(VI) Ions on Magnetite (Fe_3O_4) Nano-Particles: Kinetic and Thermodynamic Studies*" El-Cezerî Journal of Science and Engineering, 2016, 3(3);417-427.

Bu makaleye atıf yapmak için
Çiftçi, H., Ersoy, B. *"Cr(VI) İyonlarının Manyetit (Fe_3O_4) Nano-Partikülleri Üzerine Adsorpsiyonu: Kinetik ve Termodinamik Çalışmalar"* El-Cezerî Fen ve Mühendislik Dergisi 2016, 3(3);417-427.

1. Introduction

Chromium is a heavy metal which has toxic effect and used in various applications such as chromium-plating, production of chromium alloys or metals, leather, ceramic, glass, paint and ink industries [1, 2]. Hexavalent chromium [Cr(VI)] and trivalent chromium [Cr(III)] are two main forms of chromium most occurring in the aquatic environment. Most of the components of Cr(VI) has been reported to be toxic and carcinogenic [3, 4]. Unlike other chromium components, Cr(VI) is soluble in water and therefore its transportation and participation to living organisms are much more likely. According to the World Health Organization (WHO) standards, maximum allowable Cr(VI) concentration in drinking waters is 0.05 mg/l [5-7]. Thus, the amount of chromium content in the waste waters which have dangerous effect on living beings should be reduced to a minimum level before releasing in to the environment.

Magnetite nano-particles (MNPs) are of great interest as a new adsorbent in recent years to remove heavy metals from waste waters which have some advantageous properties such as high surface area and high magnetic sensitivity [8]. With these features, MNPs have high adsorption capacity for heavy metals and easily separable by an external magnetic field from aqueous media. Furthermore, MNPs are also used for some specific applications such as drug delivery, magnetic field-assisted cancer therapy, magnetic resonance imaging and sensing. These applications require that the nanoparticles are superparamagnetic with sizes smaller than 20 nm to have uniform physical and chemical properties.

In this study, adsorption technique which is economic, efficient and easier technique for application was used to remove Cr(VI) ions from aqueous media by MNPs. After adsorption experiments kinetic and thermodynamic properties of Cr(VI) adsorption by MNPs were investigated.

2. Materials and Methods

2.1. Materials

Iron(III) chloride ($FeCl_3.6H_2O$, >98%), iron(II) chloride ($FeCl_2.4H_2O$, >99%), hydrochloric acid (HCl, %35-37 GR), sodium hydroxide (NaOH, 96%), sulphuric acid (H_2SO_4, 95-97%), potassium dichromate ($K_2Cr_2O_7$), acetone (C_3H_6O) and ethanol (C_2H_5OH, 99.7%) were purchased from Merck. Ammonium hydroxide (NH_4OH, 28-30%) and 1,5-Diphenylcarbazide (DPC, $C_{13}H_{14}N_4O$) were purchased from Sigma Aldrich.

A stock solution of 500 mg/l Cr(VI) was prepared by dissolving of 1.414 gr $K_2Cr_2O_7$ with 1000 ml distilled water. 1.5-DPC (0.5%) solution was used for UV measurements and prepared by dissolving of 0.25 gr 1.5-DPC with 50 ml acetone. 6 N sulphuric acid solution was prepared by adding 8.33 ml H_2SO_4 (98%) into 50 ml distilled water to be used to pH adjustments at UV measurements.

MNPs with an average particle size of 15 nm were synthesized according to our previous report using chemically co-precipitation technique [9].

2.2. Adsorption Experiments

Batch adsorption experiments were performed in a 100 ml erlenmayer flask with 50 ml Cr(VI) solution of known concentration and desired amount of adsorbent. The mixture was stirred using a GFL-1086 shaking water bath at 175 rpm. After that the adsorbent was taken from solution by

magnetic separation using a magnet and the solution analyzed for the residual Cr(VI) determination by Shimadzu UV-1240 spectrophotometer. Figure 1 shows a schematic summary of adsorption and Cr(VI) determination experiments.

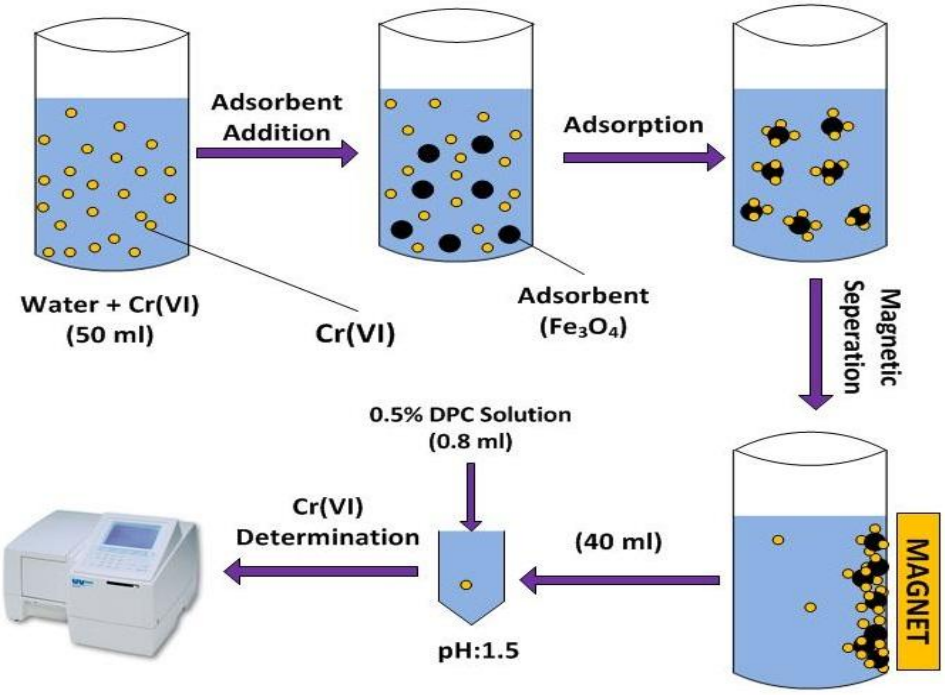

Figure 1. Schematic illustration of adsorption process and Cr(VI) determination experiments.

The percentage removal of Cr(VI) and amount of adsorption at equilibrium, qe (mg/g), were calculated by using following Equations 1 and 2.

$$\text{Removal}(\%) = \frac{C_i - C_e}{C_i} 100 \quad (1)$$

$$q_e = \frac{C_i - C_e}{m} V \quad (2)$$

where C_i and C_e are initial and final concentration of Cr(VI) (mg/l) in the solution, respectively. V is the volume (l) of tested solution and m is the mass of used adsorbent (g).

2.3. Determination of Cr(VI) Ions

The amount of Cr(VI), remained in solution after adsorption experiments, was determined using UV-vis spectrophotometer and the used method is as follows; 40 ml of sample was taken in a beaker and 3 ml of 6 N H_2SO_4 was added into the solution to decrease the pH of the solution under 2. Then 0.8 ml of 0.5% DPC solution was added in the mixture. After waiting 5 minutes, the UV measurements were performed [10].

3. Results and Discussion

3.1. Adsorbent Characterization

Figure 2 shows the XRD pattern of MNPs. Large peaks show nano-crystalline and sharp peaks show the high degree of crystalline structure [11]. As can be seen in the figure, crystalline diffraction peaks with 2θ at 30.1°, 35.4°, 43.2°, 53.9°, 57.2° and 62.7° correspond to the characteristic planes [(220), (311), (400), (422), (511), (440)] of cubic spinel Fe_3O_4, respectively (JCPDS No. 01-071-6336).

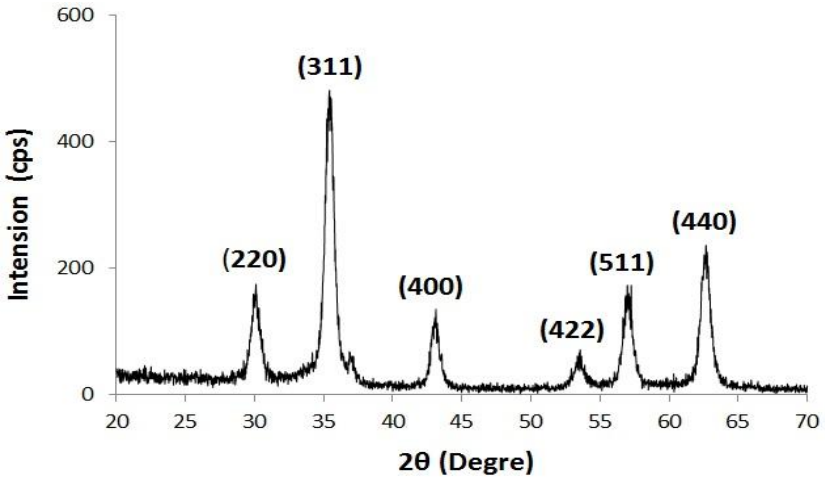

Figure 2. XRD pattern of MNPs

Mean crystallite size and lattice constant of MNPs were calculated according to the Scherrer's formula given in the Equations 3 and 4, respectively. The calculated results are demonstrated in the Table 1.

$$D_{XRD} = \frac{k\,\lambda}{\beta\,Cos(\theta)} \tag{3}$$

$$\alpha = d_{hkl}\,[h^2 + k^2 + l^2]^{1/2} \tag{4}$$

where k is the particle shape factor (0.89 for magnetite), λ is the X-ray wavelength (0.15406 nm), β is the full width at half height of the diffraction peak (radian), θ is the Bragg diffraction angle (17.75), d_{hkl} is the crystal plane space ($d_{hkl} = \lambda/2Sin\theta$) and h, k, l are the Miller index.

Table 1. Structural XRD parameters obtained for (3 1 1) basic plane.

2θ (der)	β (der)	D_{XRD} (nm)	α (nm)	d_{hkl} (nm)
35.42	0.734	11.24	0.8397	0.2532

TEM images of the MNPs were shown in Figure 3. The average size of MNPs was estimated to be 15 nm and MNPs has approximately spherical shape as seen in the figure.

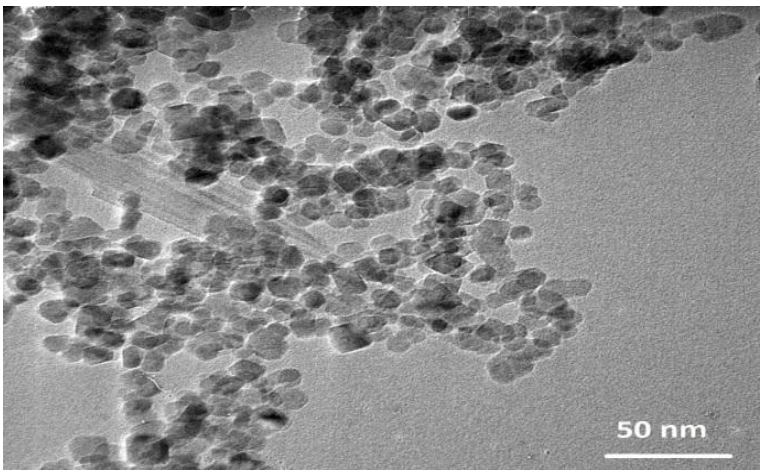

Figure 3. TEM micrograph of MNPs.

Magnetization curve of synthesized MNPs is given in the Figure 4. Magnetization saturation (M_s) of MNPs was found to be 75 $emug^{-1}$. Additionally, the magnetization curve has gone through exactly the origin of magnetization graph. This means that the synthesized MNPs show superparamagnetic behavior at room temperature because of not exhibiting hysteresis, coercivity and remanence [12].

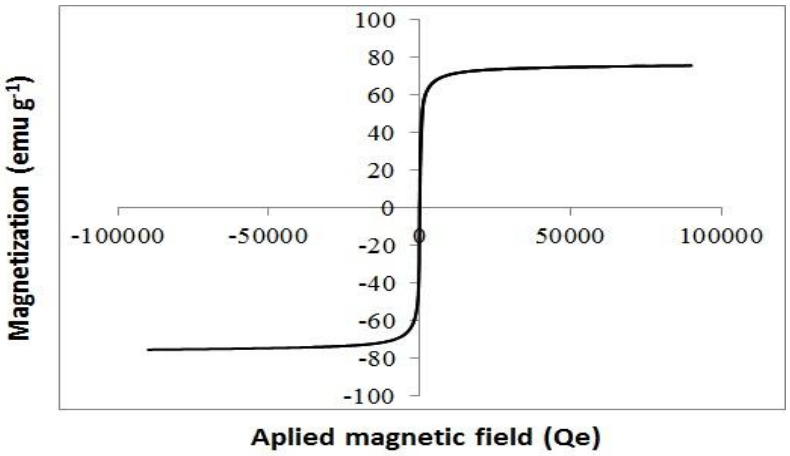

Figure 4. Magnetization curve of MNPs.

3.2. Adsorption Kinetics

Figure 5 shows the change in adsorption capacity for 5-25 mg/l initial Cr(VI) concentrations and times up to 150 minutes. As it is expected, a rapid increasing of the adsorption capacity was shown in the first stage and then slowed down until it reaches the equilibrium time. The adsorption capacity increased from 17.4 mg/g to 24.9 mg/g when percentage removal decreased from 87.5% to 62.2% by increasing of the initial Cr(VI) concentration from 10 mg/l to 20 mg/l. This situation can be explained by the mass transfer rate resulted from growing driving force [13]. Additionally, the curves reaches an equilibrium at 90 minutes and initial Cr(VI) concentration has no effect on the equilibrium time. According to these results, it can be said that the adsorption of Cr(VI) on the surface of MNPs is monolayer [14].

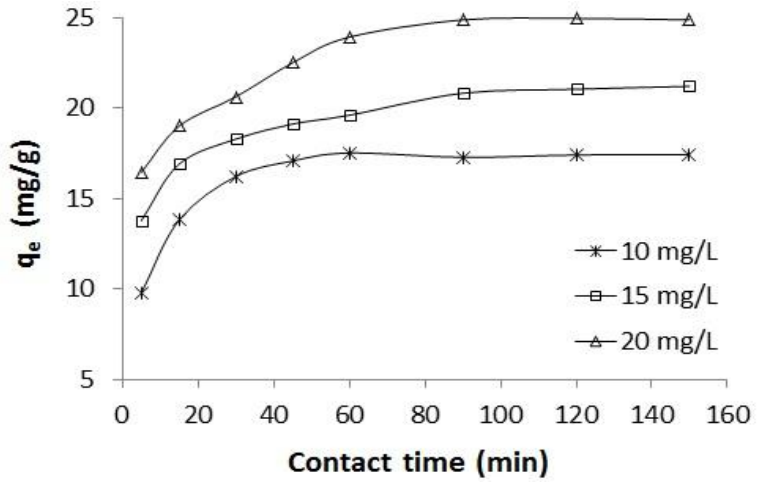

Figure 5. Effect of contact time and initial Cr(VI) concentration on the removal of Cr(VI) by MNPs (adsorption conditions: amount of adsorbent, 0.5gL^{-1}; temperature, 25 ^{o}C; pH, 3).

In order to investigate the adsorption mechanism, the data were fitted to pseudo-first-order and pseudo-second-order kinetic models. Linear forms of first and second order models were given in the Equations 5 and 6, respectively [15].

$$log(q_e - q_t) = log(q_e) - \frac{k_1}{2.303} t \quad (5)$$

$$\frac{t}{q_t} = \frac{1}{h} + (\frac{1}{q_e})t \qquad (h=k_2 qe^2) \quad (6)$$

$k_1/2.303$ and $\log(q_e)$ values were found from slope and intercept of the plot of $\log(q_e-q_t)$ versus t (Figure 6a). $1/q_e$ and $1/k_2qe^2$ values were found from slope and intercept of the plot of t/q_t versus t (Figure 6b). The obtained reaction rate constants (k_1 and k_2), adsorption capacities (mg/g) and R^2 values are shown in the Table 2.

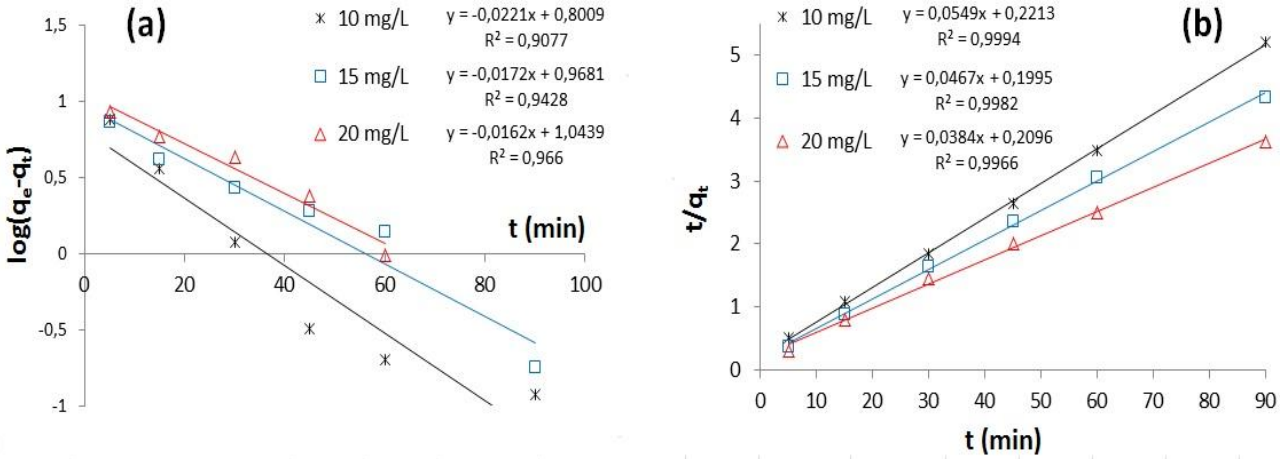

Figure 6. Kinetic models for adsorption of Cr(VI) by MNPs; (a) pseudo-first-order kinetic model, (b) pseudo-second-order kinetic model.

According to Table 2, the calculated adsorption capacities ($q_{e,cal}$) from pseudo-second-order model are very close to the experimental adsorption capacity ($q_{e,exp}$) values. When viewed correlation coefficients, the pseudo-second-order model (R^2: 0.997–0.999) have a better description of the

Cr(VI) adsorption compared to pseudo-first-order model (R^2: 0.908–0.966). Therefore, it is clear that adsorption of Cr(VI) on the MNPs follows the pseudo-second-order kinetic model.

Table 2. Kinetic parameters for adsorption of Cr(VI) onto the Fe_3O_4 NPs.

C_0 (mg/l)	$q_{e,exp}$ (mg/g)	Pseudo-first-order			Pseudo-second-order		
		k_1, (1/dk)	$q_{e,cal}$ (mg/g)	R^2	k_2 (g/mgdk)	$q_{e,cal}$ (mg/g)	R^2
10	17.4	0.0509	6.32	0.908	0.01363	18.21	0.999
15	21.0	0.0396	9.29	0.943	0.01094	21.41	0.998
20	24.9	0.0373	11.06	0.966	0.00704	26.04	0.997

3.3. Adsorption Thermodynamic

Effect of temperature on Cr(VI) removal as a function of initial chromium concentration is illustrated in the Figure 7. As seen clearly from figure, the adsorption capacity (mg/g) increased with increasing of temperature and this result indicates that the adsorption of Cr(VI) on MNPs is a endothermic process.

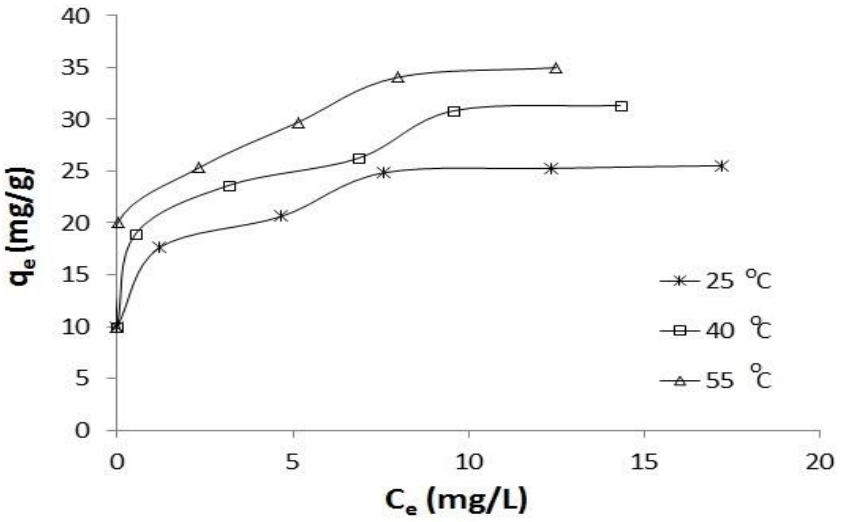

Figure 7. Effect of temperature on the removal of Cr(VI) by MNPs (adsorption conditions: initial concentration of Cr(VI), 10 mg/l; contact time, 90 min; adsorbent concentration, 0.5gL^{-1}; pH, 3)

Thermodynamic parameters which Geebs free energy (ΔG^o), enthalpy change (ΔH^o) and entropy change (ΔS^o) can be calculated according to Equations 7-9. $-\Delta H^0/R$ and $\Delta S^0/R$ values were found from slope and intercept of the plot of 1/T versus $\ln K_c$ given in the Figure 8.

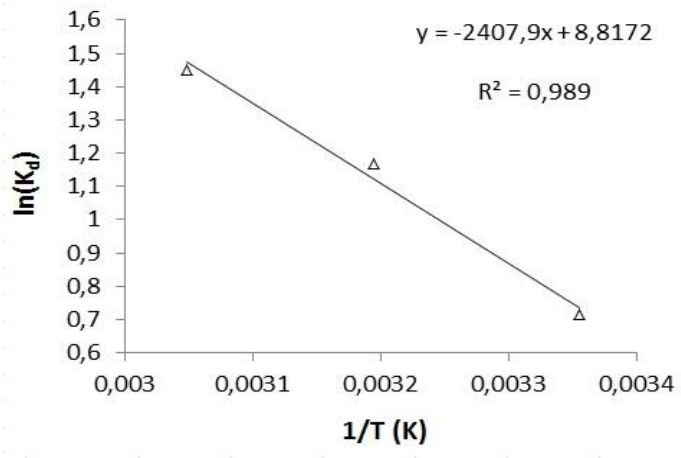

Figure 8. Van't Hoff plot for Cr(VI) adsorption by MNPs.

Thermodynamic parameters are shown in the Table 3. Negative ΔG^o shows that the adsorption process is spontaneous and feasible, positive ΔH^o values are a result of endothermic reactions and the negative values of ΔS^o indicate a decreased randomness at the solid/solution interface during the adsorption process.

$$K_c = C_{ads} / C_e \quad (7)$$

$$\Delta G^0 = -RTlnK_d \quad (8)$$

$$lnKc = \frac{\Delta S^0}{R} - \frac{\Delta H^0}{RT} \quad (9)$$

where K_c is the equilibrium constant, C_e is the equilibrium concentration in solution (mg/l) and C_{ads} is the solid phase concentration at equilibrium (mg/l), R is the gas constant (8.314 J/mol K) and T is the absolute temperature (K).

Table 3. Thermodynamic parameters for adsorption of Cr(VI) by MNPs.

Temperature (^oC)	ΔG^o (J mol^{-1})	ΔH^o (J mol^{-1})	$-\Delta S^o$ (J $mol^{-1}K^{-1}$)
25	-1772.82		
40	-3042.42	23449.9	84.0
55	-3960.79		

3.3. Adsorption Isotherms

Figure 9 shows the adsorption isotherms of Cr(VI) removal by MNPs at temperatures 25^{o}C, 40^{o}C and 55^{o}C. Langmuir and Freundlich models were employed to investigate the isotherm data. The linearized Langmuir isotherm model is represented by Equation 10 [16]. Dimensionless separation factor (R_L) which given by Equation 11 is essential for Langmuir model to define the favorability of an adsorption process [15]. The linear form of Freundlich model is expressed by Equation 12 [18].

$$\frac{C_e}{q_e} = \frac{1}{q_{m^*}\, b} + \frac{1}{q_m} C_e \quad (10)$$

$$R_L = \frac{1}{1+(b*C_o)} \tag{11}$$

$$\ln(q_e) = \ln(K_f) + \frac{1}{n}\ln(C_e) \tag{12}$$

where q_m (mg/g) is the maximum adsorption capacity, b (l/mg) is the Langmuir constant, K_f and 1/n constants are related to the adsorption capacity and intensity of adsorption, respectively.

$1/q_m$ and $1/q_m b$ values were found from slope and intercept of the plot of C_e/q_e versus C_e (Figure 9a) and 1/n and $\ln(K_f)$ values were found from slope and intercept of the plot of $\ln(C_e)$ versus $\ln(q_e)$ (Figure 9b). The isotherm constants and correlation coefficients are shown in the Table 4 and according to the correlation coefficients (R^2), adsorption isotherms of the used adsorbent for removal of Cr(VI) could be better described by the Langmuir model than by the Freundlich model.

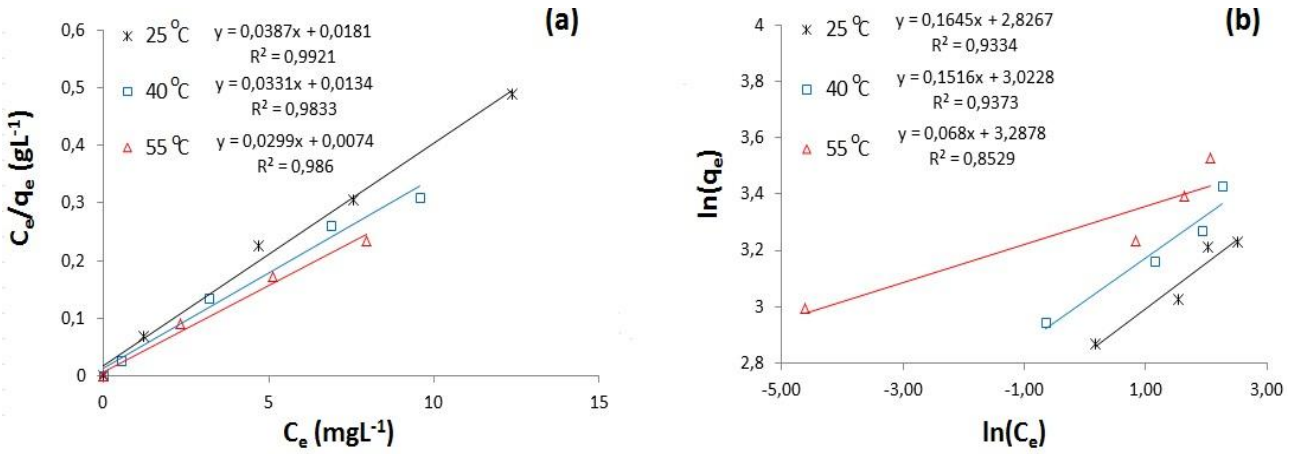

Figure 9. Linear forms of Langmuir (a) and Freundlich (b) isotherms.

As a result we can say that the adsorption of C(VI) ions on MNPs was happened in monolayer. Namely, adsorption occurs on the specific homogeneous areas of adsorbent surface and each of these areas is occupied by only one metal ion, more of these ions cannot be adsorbed. The maximum capacity of adsorbent (q_m) which in the range of 25.84-33.45 mg/g was calculated from the Langmuir plots. Additional, increased adsorption capacity with increasing of the temperature proved the endothermic reactions of adsorption process. The equilibrium parameter (R_L) was found to be in the range $0<R_L<1$ shown in the Table 4. This proves that the adsorption process is favorable as desired level [2].

Table 4. Langmuir and Freundlich isotherm constants for adsorption of Cr (VI) by MNPs.

Temperature (°C)	Langmuir constants				Freundlich constants		
	q_m (mg/g)	b (l/g)	R_L	R^2	K_f (mg/g)	n	R^2
25	25.84	2.14	0.045	0.992	16.89	6.08	0.933
40	30.21	2.47	0.039	0.983	20.55	6.60	0.937
55	33.45	4.04	0.024	0.986	26.78	14.71	0.853

4. Conclusion

Fe_3O_4 nano-particles (MNPs) have been shown to be an effective adsorbent for removal of Cr(VI) ions from aqueous media. Electrostatic attraction forces between Cr(VI) ions and MNPs play a key role for this adsorption process. Maximum Cr(VI) adsorption capacity was found to be 33.45 mg/g with 88% removal at pH 3.0. Thermodynamic calculations showed that the Cr(VI) adsorption by MNPs is endothermic and spontaneous in nature. The adsorption data were fitted well with Langmuir isotherm and the kinetics of the adsorption followed the pseudo-second-order model. According to these results, MNPs can be used as an effective adsorbent for removal of Cr(VI) ions from industrial waste waters. Additionally, we can say that the magnetic separation of MNPs from solution is more rapid, simpler and more effective than other solid-liquid separation techniques.

References

[1] Slooff, W., "Integrated criteria document chromium"," Bilthoven, Netherlands, National Institute of Public Health and Environmental Protection, (Report no. 758701002) (1989).

[2] Chiou, M.S., "Equilibrium and kinetic modeling of adsorption of reactive dye on cros linked chitosan beads", Chemosphere, 50 (2002) 1095-1105.

[3] Sikaily, A.E., Nemr, A.E., Khaled, A. and Abdelwehab, O., "Removal of toxic chromium from wastewater using green alga Ulva lactuca and its activated carbon", J. Hazard. Mater, 148 (2007) 216–228.

[4] Li, H., Li, Z., Liu, T., Xiao, X., Peng, Z. and Deng, L., "A novel technology for biosorption and recovery hexavalent chromium in wastewater by bio-functional magnetic beads", Bioresour. Technol, 99 (2008) 6271–6279.

[5] World Health Organization (WHO), "Guidelines for drinking-water quality", 3rd ed., (2004) 1:334, Geneva

[6] World Health Organization (WHO), "Chromium, Environmental Health Criteria", No:61 (1988) Geneva.

[7] Dhungana, T.P. and Yadav, P.N., "Determination of Chromium in Tannery Effluent and Study of Adsorption of Cr(VI) on Sawdust and Charcoal from Sugarcane Bagasses", J. Nepal Chem. Soc., 23 (2009) 2008/2009.

[8] Ngomsik, A.F, Bee, A., Draye, M., Cote, G., Cabuil, V., Magnetic nano and microparticles for metal removal and environmental applications: a review, Comptes Rendus Chimie, 8(6–7) (2005) 963-970.

[9] Çiftçi, H., Ersoy, B., Evcin, A., "Synthesis and Characterization of Superparamagnetic Magnetite/Modified Magnetite Nano-Particles (Fe_3O_4@SiO_2@L)", Nano Materials for Energy and Environment (NanoTech 2016), 01- 03 June 2016, Paris – France.

[10] APHA, "Standard Methods For the Examination of Water and Wastewater", 19 th Ed., American Public Health Association, Washington DC. (1995).

[11] Farimani, M.H., Shahtahmasebi, N., RezaeeRoknabadi, M., Ghows, N. and Kazemi, A., "Study of structural and magneticproperties of superparamagnetic Fe_3O_4/SiO_2 core–shell nano composites synthesized with hydrophilic citrate-modified Fe_3O_4 seeds via a sol–gel approach", Physica E, 53 (2013) 207–216.

[12] Zhao, X., Shi, Y., Wang, T., Cai, Y., Jiang, G., "Preparation of silica-magnetite nanoparticle mixed hemimicelle sorbents for extraction of several typical phenolic compounds from environmental water samples", Journal of Chromatography A, 1188 (2008) 140–147.

[13] Garg, U.K., Kaur, M.P., Garg, V.K. and Sud, D., "Removal of nickel (II) from aqueous solution by adsorption on agricultural waste biomass using a response surface methodological approach", Bioresour. Technol., 99(5) (2008) 1325–1331.

[14] Namasivayam, C., Sangeetha, D., "Recycling of agricultural solid waste coir pith: removal of anions, heavy metals, organics and dyes from water by adsorption onto $ZnCl_2$ activated coir pith carbon", J. Hazard. Mater., 135 (2006) 449–452.

[15] Hamadi, N.K., Chen, X.D., Farid, M.M. Lu, M.G.Q., "Adsorption kinetics for the removal of chromium (VI) from aqueous solution by adsorbents derived from used tyres and sawdust", Chem. Eng. J. 84 (2001) 95–105.

[16] Langmuir İ., "The adsorption of gases on plane surfaces of glass, mica and platinum", Journal of American Chemical Society, 40(9) (1918) 1361-1403.

[17] Masel, A.I., "Principles of adsorption and reaction on solid surfaces", Wiley, New York (1996).

[18] Freundlich, H.M.F., "Over the adsorption in solution", Journal of Physical Chemistr, 57(385) (1906) 292.